

The total number and mass of SARS-CoV-2 virions in an infected person

Ron Sender^{1*}, Yinon M. Bar-On^{1*}, Avi Flamholz², Shmuel Gleizer¹, Biana Bernstein^{1,5}, Rob Phillips^{3,4}, Ron Milo¹

¹Weizmann Institute of Science, Rehovot 7610001, Israel

²University of California, Berkeley, CA 94720, USA

³California Institute of Technology, Pasadena, CA 91125, USA

⁴Chan Zuckerberg Biohub, 499 Illinois Street, SF CA 94158, USA

⁵Present address: Ragon Institute of MGH, MIT and Harvard, Cambridge, MA 02138, USA

* Equal contribution

Quantitatively describing the time course of the SARS-CoV-2 infection within an infected individual is important for understanding the current global pandemic and possible ways to combat it. Here we integrate the best current knowledge about the abundance of potential SARS-CoV-2 host cells and typical concentrations of virions in bodily fluids to estimate the total number and mass of SARS-CoV-2 virions in an infected person. We estimate that each infected person carries 10^9 - 10^{11} virions during peak infection, with a total mass of about 1 μ g-0.1 mg, which curiously implies that all SARS-CoV-2 virions currently in the world have a mass of only 0.1-1 kg. Knowledge of the absolute number of virions in an infected individual can put into perspective parameters of the immune system response, minimal infectious doses and limits of detection in testing.

Estimating key biological quantities such as total number and mass of cells in our body or the biomass of organisms in the biosphere in absolute units helps develop a deep quantitative perspective and improves our intuition and understanding of the living world ([Moran et al. 2010](#); [Sender et al. 2016a](#); [Sender et al. 2016b](#); [Bar-On et al. 2018](#)). Such a quantitative perspective could help the current intensive effort to study and bring under control the COVID-19 pandemic by clarifying a myriad of key numbers such as minimal infectious doses and limits in testing. We have recently compiled quantitative data at the virus level as well as at the community level to help communicate state-of-the-art knowledge to both the public and researchers and provide them with a quantitative toolkit to think about the pandemic ([Bar-On et al. 2020](#)). Here we leverage such quantitative information to estimate the total number and mass of SARS-CoV-2 virions present in an infected individual during the peak of the infection.

Viral concentrations and viral particles are being measured in several different ways resulting in great differences in values and their meanings. Here, we report our estimates in two ways. First via viral RNA copies, as they are measured by RT-PCR, and representing the amount of viral RNA produced, including defective and deactivated virions. The second way is by infectious virions, excluding the defective and deactivated virions, measured in units of fifty-percent tissue culture infective dose (TCID₅₀) by virus titer (endpoint dilution assay quantifying the amount of virus required to kill 50% of infected host cells). Thus, we try to estimate both the total amount of viral particles through RNA copies and the number of infectious virions through TCID₅₀ measurements.

To estimate the total number of virions present in an infected individual at the peak of the infection, we rely on several studies which measured the concentration of virions (measured in genome copies per gram tissue) in tissues of rhesus macaques, after infections with SARS-CoV-2 ([Munster et al. 2020](#); [Williamson et al. 2020](#)). The viral concentrations were analyzed for samples of all the relevant tissues of the respiratory, digestive and immune systems, and were given per gram of tissue. An estimate for the total number of virions can be obtained from these measurements by multiplying the viral concentration of each tissue by the total tissue mass ([ICRP 2002](#); [Snyder et al. 1975](#)). The lungs are the largest tissue in terms of mass ($M_{lungs} \approx 1\text{kg}$) and had the highest viral concentration ($C_{virions}^{lungs}$) and thus contribute the most to the overall estimate, with

$$C_{virions}^{lungs} \times M_{lungs} = N_{virions} \quad (1)$$
$$10^6 - 10^8 \left[\frac{RNA \text{ copies}}{g} \right] \times 1 [kg] \times 1000 \left[\frac{g}{kg} \right] = 10^9 - 10^{11} [RNA \text{ copies}].$$

Other tissues, like the nasal mucosa, larynx, bronchial tree and adjacent lymph nodes all have a combined mass of ~100g and maximal concentrations of 10⁶-10⁷ RNA copies/ml and hence contribute at most an additional 10% to the estimate based on the lungs (Figure 1).

Another study ([Rockx et al. 2020](#)) measured the viral concentrations in tissues taken from infected rhesus macaques, a few days after inoculation. However, this study reports its values in units of TCID₅₀ which give an assessment of the concentration of infectious viruses. The study reports much smaller maximal values of 10³-10⁴ TCID₅₀/ml for lung tissue. Combining their concentration with the volume of an adult human lungs, we get an estimate of 10⁵-10⁷ TCID₅₀ virions in an adult, compared with 10⁹-10¹¹ RNA copies, estimated from ([Munster et al. 2020](#))(Figure 1). This large difference appears to

be representative of the use of viral titers instead of viral loads, as a similar difference of 4-5 orders of magnitude is observed in bronchoalveolar lavage fluid measurements in rhesus macaques by (Williamson et al. 2020) and in nasopharyngeal swabs taken from 454 human participants (Quicke et al. 2020).

Based on this line of evidence, we estimate the total number of virions in an infected individual during peak infection at 10^9 - 10^{11} RNA copies, or 10^5 - 10^7 TCID₅₀.

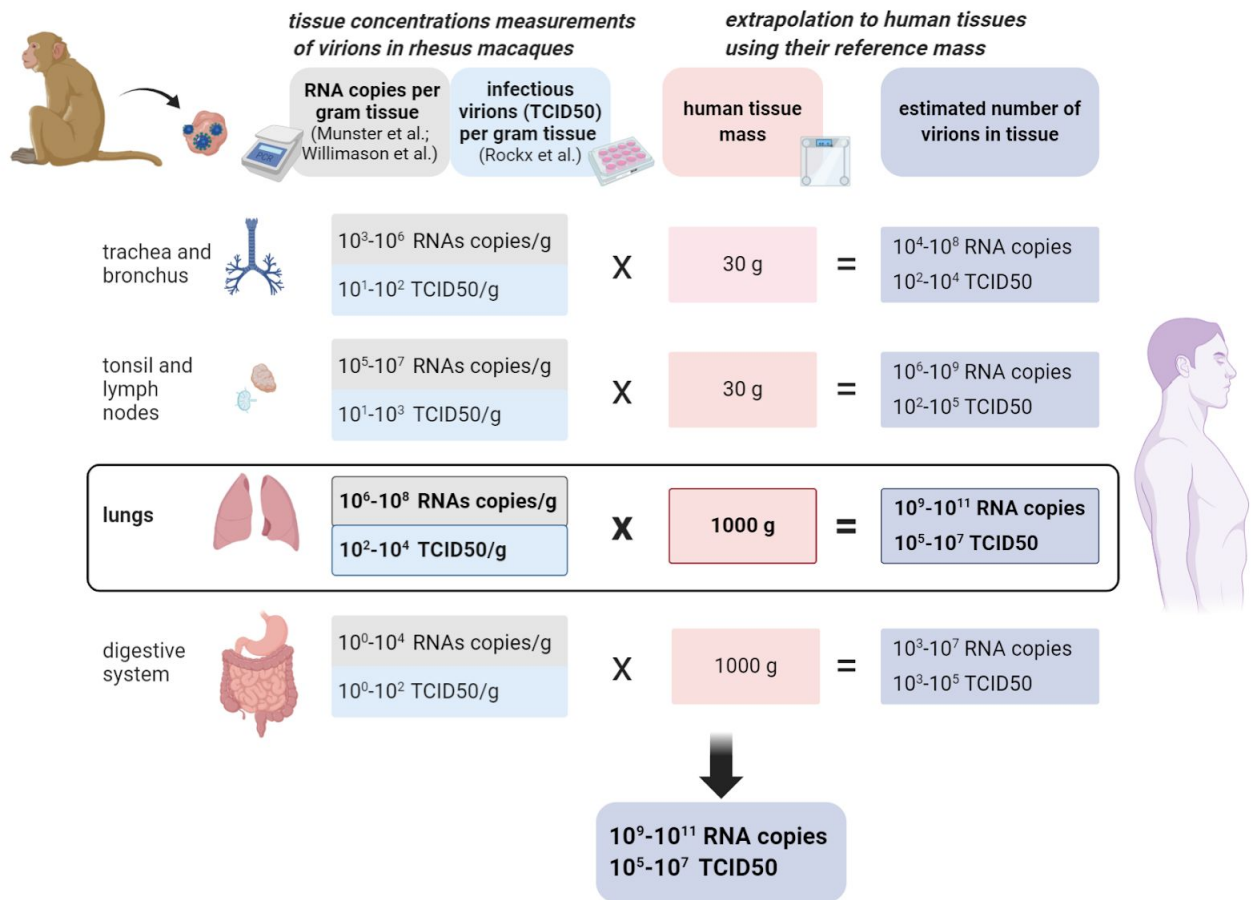


Figure 1: A schematic representation of the estimate of the number of virions in an infected individual. The estimate is made using the concentrations of virions measured in a gram of rhesus macaque tissue multiplied by the mass of human tissues.

Calculating the total number of cells infected with SARS-CoV-2

We can leverage our estimate of the total number of virions in the body of an infected individual to estimate the size of the population of cells which are infected with the virus during peak infection. As shown in Figure 2, to estimate the total number of infected cells, we need to know how many virions are found within each infected cell.

In order to determine the number of virions within an infected cell at any given time we rely on several lines of evidence. The first is data regarding the burst size of other betacoronaviruses (as we are not aware of measurements for SARS-CoV-2). The burst size is defined as the total number of viruses produced by an infected cell (the yield) throughout its lifetime, in analogy with bacterial lytic infections. Two previous studies suggested virion yield of either 10-100 or 600-700 infectious virions (in Plaque Forming units - PFUs) ([Robb and Bond 1979](#); [Hirano et al. 1976](#)). The time scale that is relevant for this yield is a few days ([Chu et al. 2020](#)). Thus, we can assume that by the first estimate at any given moment there are few to tens infectious virions that reside in each infected cell, and tens to hundreds of infectious virions by the second. The second line of evidence concerns the density of viral particles, within a single cell. Several studies have used transmission electron microscopy (TEM) to characterize the dynamics of viral infection within cells ([Imai et al. 2020](#); [Kim et al. 2020](#); [Klein et al. 2020](#); [Ogando et al. 2020](#)). Using seven TEM scans taken from those studies we estimated that the density of viral particles within infected cells is 10^5 viral particles per 1 pL. As the human cells targeted by SARS-CoV-2 have a volume of ≈ 1 pL (resulting in a cellular mass of ≈ 1 ng) ([Stone et al. 1992](#); [Crapo et al. 1982](#)), the TEM scans indicate that at a given moment there are $\approx 10^5$ viral particles within a single cell. Those viral particles include defective virions, and as we saw earlier, it is reasonable to assume that only 1 in 10^4 of them is infective. Thus TEM scans indicate that ≈ 10 infectious virions reside inside a cell in a given moment. We can perform a sanity check using mass considerations to see that our estimate of the number of viral particles is not beyond the maximal amount that is feasible. Each viral particle has a mass of ≈ 1 fg ([Bar-On et al. 2020](#)). Hence, 10^5 viral particles weigh ≈ 0.1 ng, about 10% of the total mass of the cell (and more than a third of its dry weight). That means that it is not reasonable to assume that there are more than 10^5 viral particles or 10 infectious virions within a cell at any given moment. Following those lines of evidence we conclude that at a given moment there are ≈ 10 infectious virions residing inside a cell, and that the overall yield of an infected cell is 10-100 infectious virions over a few days.

$$\frac{N_{\text{infectious virions}}}{Y_{\text{virions per cell}}} = N_{\text{infected cells}} \quad (2)$$
$$\frac{10^5 - 10^7 [\text{virions}]}{10 [\frac{\text{virions}}{\text{cell}}]} = 10^4 - 10^6 [\text{cells}] .$$

How does this estimate stack up against the number of potential host cells for the virus? The best-characterized route of infection for SARS-CoV-2 is through cells of the respiratory system, specifically the pneumocytes (a total of about $\sim 10^{11}$ cells in the body), alveolar macrophages ($\sim 10^{10}$ cells) and the mucus cells in the nasal cavity ($\sim 10^9$

cells) ([Stone et al. 1992](#); [Crapo et al. 1982](#)). Other cell types, like enterocytes (gut epithelial cells) can also be infected ([Lamers et al. 2020](#)). Our best estimate for the size of the total potential pool of host cells is thus $\sim 10^{11}$ cells, and the fraction of cells infected during peak infection therefore represents a small fraction of this potential pool (1 in 10^5 - 10^7).

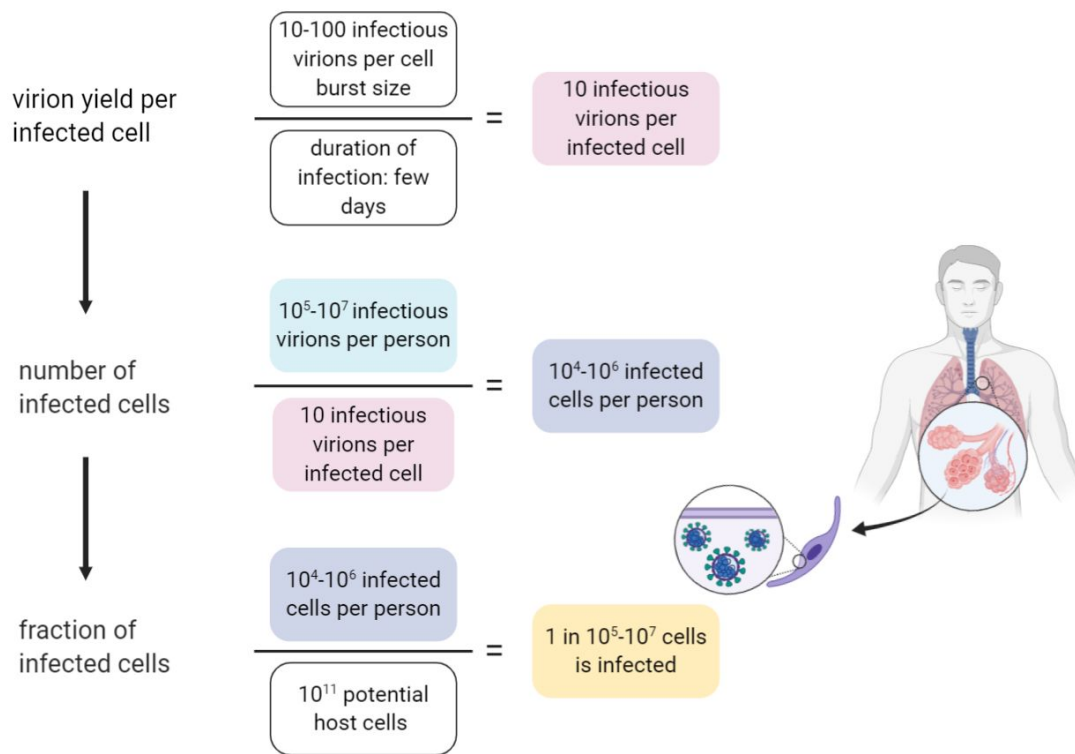


Figure 2: Estimation of the number of infected cells and their fraction out of the potential relevant host cells.

Virion production rate and the total number of virions produced throughout an infection

In addition to analyzing the state of an infected individual during peak infection, we can also ask what is the total number of virions produced over the course of an infection, as well as what is the rate of virion production inside a human host. First, in order to estimate the total number of virions produced during an infection, we rely on the average number of viruses an infected cell yields, which is about 10-100 (based on measurements from different kinds of betacoronavirus ([Robb and Bond 1979](#); [Hirano et al. 1976](#)), and our estimate of the number of virions within a single cell at any given moment). The total number of virions produced over the course of an infection can be

estimated by multiplying the burst size by the total cumulative number of infected cells as

$$\begin{aligned} N_{cells} \times Y_{virions\ per\ cell} &= \widehat{N}_{total\ virions\ throughout\ disease} \\ 10^4 - 10^6 [cells] \times 10 - 100 [\frac{virions}{cell}] &= 10^5 - 10^8 [infectious\ virions, TCID50] \end{aligned} \quad (3)$$

This value exceeds the peak number of virions we estimated by about an order of magnitude. In terms of RNA copies, this translates into 10^9 - 10^{12} RNA copies.

In order to estimate the rate of production of virions we divide the burst size by the duration it takes the infected cells to produce that burst size, known to be a few days ([Bar-On et al. 2020](#)). We thus estimate that each infected cell produces ~10 infectious virions per day on average. To estimate the maximal production rate for all infected cells, we multiply this production rate per single infected cell by the 10^4 - 10^6 infected cells. Thus the maximal production rate of virions is given by:

$$\begin{aligned} N_{cells} \times Q_{virions\ per\ cell\ per\ day} &= P_{virions\ per\ day} \\ 10^4 - 10^6 [cells] \times 10 [\frac{virions}{cell \times day}] &= 10^5 - 10^7 [\frac{infectious\ virions\ (TCID50)}{day}]. \end{aligned} \quad (4)$$

While the estimates were performed using a reference value for the lung mass taken from adult men, they can be generalized for women and children. We rely on the multiplication of the viral concentration in the lungs and the total mass of the lungs. Reference values for the lung mass show a value smaller by 20% for women, and 75%-25% for children aged 5-15 years ([ICRP 2002](#)). Although COVID-19 is known to affect adult men more than women and children ([Salje et al. 2020](#); [WHO 2020](#)), there is scarce information regarding difference in viral concentrations across gender and age. One preprint ([Jones et al. 2020](#)) suggests that viral concentration in children is lower by up to an order of magnitude, but the change they measured is not consistent across the entire age range. Assuming the change in measured viral load represents a similar change in viral concentration in the lung tissue, and combining the concentrations with the reduced lung mass, we get that the number of virions in an infected woman is similar to that estimated for men, and that an infected child is probably carrying an order of magnitude less virions.

Discussion

To provide some context for our estimate of the total number of virions per infected individual, we can compare it with the total of 3×10^{13} human cells in the body ([Sender et al. 2016b](#)). We find that even for the higher end of the range of estimates for viral particles there is still a 10-100 factor in favor of the human cells. A more functional comparison is with the number of antibodies the body produces to combat the viral infection. Total IgG antibody levels specific for SARS-CoV-2 spike protein (C_{IgG}) were measured 3 weeks following symptom onset showing a concentration in the serum on the order of $\sim 10 \mu\text{g/mL}$ ([Iyer et al. 2020](#)). Only a fraction of $\approx 5\%$ of the total anti-spike IgG antibodies has the capacity to neutralize the virus ($f_{neutralizing}$) ([Rogers et al. 2020](#)). Combining the concentration of neutralizing IgG antibodies with a mean IgG molecular weight (MW_{IgG}) of 150 kDa ([Janeway et al. 2001](#)) we can derive the number of neutralizing antibody molecules in an mL of serum ($\hat{N}_{neutralizing}$):

$$C_{IgG} \times f_{neutralizing} \times \frac{1}{MW_{IgG}} \times N_{Avogadro} = \hat{N}_{neutralizing} \quad (5)$$

$$10^{-5} \left[\frac{\text{g IgG}}{\text{mL}} \right] \times 5\% \left[\frac{\text{neutralizing}}{\text{IgG}} \right] \times \frac{1}{150,000} \left[\frac{\text{mol}}{\text{g}} \right] \times 6 \times 10^{23} \left[\frac{\text{molecules}}{\text{mol}} \right] = 3 \times 10^{12} \left[\frac{\text{neutralizing molecules}}{\text{mL}} \right].$$

Combining this estimate with the measurement of viral concentration within the lung tissue ([Munster et al. 2020](#)) and accounting for 30-40 spike trimers on each SARS-CoV-2 virion ([Yao et al. 2020](#), [Turoňová et al. 2020](#)) we can estimate the ratio of neutralizing antibodies to viral spike proteins:

$$\frac{\hat{N}_{neutralizing}}{C_{virions}^{lungs} \times N_{spike\ proteins}} = R_{neutralizing\ antibodies/spike\ proteins} \quad (6)$$

$$\frac{3 \times 10^{12} \left[\frac{\text{neutralizing molecules}}{\text{mL}} \right]}{10^6 - 10^8 \left[\frac{\text{viral particles}}{\text{mL}} \right] \times 30} = 10^3 - 10^5 \left[\frac{\text{neutralizing antibodies}}{\text{spike protein}} \right].$$

Previous work on morphologically similar viruses such as influenza and flavivirus found that a ratio of 1 neutralizing antibody to 2-4 receptor-binding proteins was sufficient to neutralize binding of a virion to its cellular receptor ([Taylor et al. 1987](#); [Pierson and Diamond 2015](#)). Taken at face value, our estimate seems to suggest an excess of neutralizing antibody molecules, even if we consider that the antibodies concentrations 30-in the lung tissue is lower than that of the blood, and the extensive glycosylation patterns found on the spike protein that shield many of its epitopes ([Turoňová et al. 2020](#)) from neutralizing antibody binding and thus decrease the efficiency of neutralization ([Schön et al. 2020](#)). However, it is important to remember that in order to estimate the effectiveness of antibody neutralization, we need to estimate the fractional occupancy of the viral epitopes by antibodies. This fractional occupancy is determined by the strength of the binding of the neutralizing antibodies to the viral particles, given

by the dissociation constant K_d ([Pierson and Diamond 2015](#)). Following the first order relation:

$$\text{fraction bound by } nAb = \frac{[nAb]}{[nAb] + K_d} \quad (7)$$

As the dissociation constants are mostly in the range of 1-10 nM ([Chi et al. 2020](#); [Seydoux et al. 2020](#)) we get:

$$[nAb] = 3 \times 10^{12} \left[\frac{\text{neutralizing molecules}}{\text{mL}} \right] \times \frac{1}{6 \times 10^{23}} \left[\frac{\text{mol}}{\text{molecules}} \right] \times 1000 \left[\frac{\text{mL}}{\text{L}} \right] = 3 \times 10^{-9} \left[\frac{\text{mol}}{\text{L}} \right] = 3 \text{ [nM]}$$

$$\text{fraction receptors bound by } nAb = \frac{3 \text{ [nM]}}{3 \text{ [nM]} + 1-10 \text{ [nM]}} = 25\% - 75\% \quad (8)$$

Thus, the concentration of antibodies is needed to ensure that enough of the epitopes are bound, regardless of the high ratio between the number of neutralizing antibodies and viral particles.

The total number of virions and their tissue concentration can also shed some light on the mechanism of action of antiviral drugs, such as Remdesivir. In their study with rhesus macaques ([Williamson et al. 2020](#)) measured a median concentration of ≈ 3 nmol of the activated drug within 1 gram of homogenized lung tissue, after six days of treatment. This is equal to 2×10^{15} molecules per 1 gram of tissue, about 7-8 orders of magnitude more than the concentration of virions within the tissue. It appears that this ratio of antiviral drug to viral concentration is needed as the reported concentrations are also close to the measured EC50 (50% effective concentration) of $\approx 10 \mu\text{M}$ ([Choy et al. 2020](#)).

One can contextualize these estimates using an absolute mass perspective. Each virion has a mass of ≈ 1 fg ([Bar-On et al. 2020](#)). Therefore even when the body carries 10^9 - 10^{11} viral particles, these have a mass of only about 1-100 μg , i.e. 1-100 times less than the mass of a poppy seed. Taking a global view across all of humanity and assuming a total of 10-100 million infected people at a given time (including the undetected), we arrive at a total mass of all the virions residing in humanity to be on the order of 0.1-1 kg. Furthermore, using the total number of viral particles produced throughout an infection (10^9 - 10^{12} per person) we can derive the total mass of all the SARS-CoV-2 viral particles ever produced throughout this current pandemic. Assuming the total number of infected people actually will be 1 billion people we find the total mass of viral particles produced for such widespread infection to be on the order of

$$N_{\text{infected people}} \times M_{\text{viral particle}} \times N_{\text{viral particles produced per person}} = M_{\text{all viral particles produced}} \quad (9)$$

$$10^9 [\text{people}] \times 10^{-15} \left[\frac{\text{g}}{\text{viral particle}} \right] \times 10^9 - 10^{12} \left[\frac{\text{viral particles produced}}{\text{person}} \right] = 1 - 1000 \text{ kg} .$$

We have shown how our estimate for the total number of virions could be used to estimate currently unknown quantities such as the fraction of potential host cells that are infected during peak infection. Single-cell RNA-sequencing studies ([Sungnak et al. 2020](#); [Zeigler et al. 2020](#); [Lukassen et al. 2020](#)) indicate that a few percent of the cells in the lungs and airways express ACE2 (angiotensin-converting enzyme 2) and TMPRSS2 (Transmembrane protease, serine 2), the receptor and main protease SARS-CoV-2 relies on for infecting cells. Most of the cells that have been found to express both are type 2 pneumocytes. While these results might be biased due to drop-out effects in measurements of only a few molecules ([Valyaeva et al. 2020](#); [Zeigler et al. 2020](#)), it is still reasonable that 1%-10% of the lung and airway cells contain the necessary receptor to be infected by SARS-CoV-2. This number is several orders of magnitude higher than our estimate for the total number of infected cells during peak infection - a fraction of 1 in 10^5 - 10^7 of the potential lung cells. This suggests that out of the cells expressing both ACE2 and TMPRSS2, only a small fraction, e.g. 10^{-3} - 10^{-5} , get infected by the virus.

There is very high variability in viral loads, exceeding 5 orders of magnitudes, as can be seen from samples taken from the upper respiratory system ([Jacot et al. 2020](#)). This wide variation reflects the difference between people as well as differences in viral load through the progression of infection within an infected individual ([He et al. 2020](#)). In our estimates we consider only a smaller range of viral concentration, corresponding to the center of the distribution of the measured values (interquartile range - between the quantiles 25%-75%). Thus, extreme cases could exceed the range provided by additional two orders of magnitudes, reaching values of 10^{13} viral particles in a single person at the peak of infection, while up to 10% of the cells expressing both ACE2 and TMPRSS2 are infected.

Major knowledge gaps that we identified are the virion yield per infected cell which is known only from a few studies on different kinds of betacoronavirus from over 40 years ago ([Robb and Bond 1979](#); [Hirano et al. 1976](#)).

The global impact of SARS-Cov-2 is clearly evident from its influence on public health and the global economy. Contrasting these global effects with the very moderate cumulative mass of these viruses highlights the limits of our day-to-day intuition in understanding and combating this pandemic and the need to rely on sound quantitative information rather than gut feelings. Having better quantitative information on the process of infection at the cellular level, the intra-host level and the inter-host level will hopefully empower researchers with better tools for thinking about ways to combat COVID-19 and curb its spread and that of future pandemics.

Acknowledgments

Gidon Eshel, Shai Fuchs, Thierry Mora, Eran Segal, Maya Shamir, Ziv Shulman, Harinder Singh, Itai Benhar, Aleksandra Walczak. Figure created using Biorender.

Funding: This research was supported by the European Research Council (Project NOVCARBFIX 646827), Israel Science Foundation (Grant 740/16), Beck-Canadian Center for Alternative Energy Research, Dana and Yossie Hollander, Ullmann Family Foundation, Helmsley Charitable Foundation, Larson Charitable Foundation, Wolfson Family Charitable Trust, Charles Rothschild, Selmo Nussenbaum, Miel de Botton (R.M.), the National Institutes of Health (1R35 GM118043-01 (Maximizing Investigators Research Award)) (R.P.) the Israeli Council for Higher Education (CHE) via the Weizmann Data Science Research Center and by a research grant from Madame Olga Klein – Astrachan (R.S.). R.M. is the Charles and Louise Gartner Professional Chair. Y.M.B. is an Azrieli Fellow

References

- Bar-on, Y.M., Flamholz, A., Phillips, R., and Milo, R. (2020). SARS-CoV-2 (COVID-19) by the numbers. *Elife*.
- Bar-On, Y.M., Phillips, R., and Milo, R. (2018). The biomass distribution on Earth. *Proc. Natl. Acad. Sci. U. S. A.* 115, 6506–6511.
- Chi, X., Liu, X., Wang, C., Zhang, X., Li, X., Hou, J., Ren, L., Jin, Q., Wang, J., and Yang, W. (2020). Humanized single domain antibodies neutralize SARS-CoV-2 by targeting the spike receptor binding domain. *Nat. Commun.* 11, 2–8.
- Choy, K.T., Wong, A.Y.L., Kaewpreedee, P., Sia, S.F., Chen, D., Hui, K.P.Y., Chu, D.K.W., Chan, M.C.W., Cheung, P.P.H., Huang, X., et al. (2020). Remdesivir, lopinavir, emetine, and homoharringtonine inhibit SARS-CoV-2 replication in vitro. *Antiviral Res.* 178, 104786.
- Chu, H., Chan, J.F.-W., Yuen, T.T.-T., Shuai, H., Yuan, S., Wang, Y., Hu, B., Yip, C.C.-Y., Tsang, J.O.-L., Huang, X., et al. (2020). Comparative tropism, replication kinetics, and cell damage profiling of SARS-CoV-2 and SARS-CoV with implications for clinical manifestations, transmissibility, and laboratory studies of COVID-19: an observational study. *The Lancet Microbe* 1, e14–e23.
- Crapo, J.D., Barry, B.E., Gehr, P., Bachofen, M., and Weibel, E.R. (1982). Cell number and cell characteristics of the normal human lung. *Am. Rev. Respir. Dis.* 125, 740–745.
- He, X., Lau, E.H.Y., Wu, P., Deng, X., Wang, J., Hao, X., Lau, Y.C., Wong, J.Y., Guan,

Y., Tan, X., et al. (2020). Temporal dynamics in viral shedding and transmissibility of COVID-19. *Nat. Med.* 26, 672–675.

Hirano, N., Fujiwara, K., and Matumoto, M. (1976). Mouse Hepatitis Virus Plaque Assay and Propagation in Mouse Cell Line DBT Cells. In *Japan. J. Microbiol.*, pp. 219–225.

ICRP (2002). Basic anatomical and physiological data for use in radiological protection: reference values. ICRP Publication 89 (Pergamon).

Imai, M., Iwatsuki-Horimoto, K., Hatta, M., Loeber, S., Halfmann, P.J., Nakajima, N., Watanabe, T., Ujie, M., Takahashi, K., Ito, M., et al. (2020). Syrian hamsters as a small animal model for SARS-CoV-2 infection and countermeasure development. *Proc. Natl. Acad. Sci. U. S. A.* 117, 16587–16595.

Iyer, A.S., Jones, F.K., Nodoushani, A., Kelly, M., Becker, M., Slater, D., Mills, R., Teng, E., Kamruzzaman, M., Garcia-Beltran, W.F., et al. (2020). Dynamics and significance of the antibody response to SARS-CoV-2 infection. *MedRxiv Prepr. Serv. Heal. Sci.* 1–31.

Jacot, D., Greub, G., Jatou, K., and Opota, O. (2020). Viral load of SARS-CoV-2 across patients and compared to other respiratory viruses. *Microbes Infect.*

Janeway, C.A.J., Travers, P., and Walport, M. (2001). The structure of a typical antibody molecule. In *Immunobiology: The Immune System in Health and Disease.*, (New York: Garland Science), pp. 1–10.

Jones, T.C., Mühlemann, B., Veith, T., Zuchowski, M., Hofmann, J., Stein, A., Edelmann, A., Corman, V.M., and Drosten, C. (2020). An analysis of SARS-CoV-2 viral load by patient age. *MedRxiv*.

Kim, J.-M., Chung, Y.-S., Jo, H.J., Lee, N.-J., Kim, M.S., Woo, S.H., Park, S., Kim, J.W., Kim, H.M., and Han, M.-G. (2020). Identification of Coronavirus Isolated from a Patient in Korea with COVID-19 Osong Public Health and Research Perspectives. *Public Heal. Res Perspect* 11, 3–7.

Klein, S., Cortese, M., Winter, S., Wachsmuth-Melm, M., Neufeldt, C., Cerikan, B., Stanifer, M., Boulant, S., Bartenschlager, R., and Chlanda, P. (2020). SARS-CoV-2 structure and replication characterized by in situ cryo-electron tomography. *BioRxiv* 1–8.

Lamers, M.M., Beumer, J., van der Vaart, J., Knoops, K., Puschhof, J., Breugem, T.I., Ravelli, R.B.G., Paul van Schayck, J., Mykytyn, A.Z., Duimel, H.Q., et al. (2020). SARS-CoV-2 productively infects human gut enterocytes. *Science* (80-.). 369, 50–54.

Lukassen, S., Chua, R.L., Trefzer, T., Kahn, N.C., Schneider, M.A., Muley, T., Winter,

H., Meister, M., Veith, C., Boots, A.W., et al. (2020). SARS -CoV-2 receptor ACE 2 and TMPRSS 2 are primarily expressed in bronchial transient secretory cells . *EMBO J.* 39, 1–15.

Moran, U., Phillips, R., and Milo, R. (2010). SnapShot: Key numbers in biology. *Cell* 141, 1–2.

Munster, V.J., Feldmann, F., Williamson, B.N., van Doremalen, N., Pérez-Pérez, L., Schulz, J., Meade-White, K., Okumura, A., Callison, J., Brumbaugh, B., et al. (2020). Respiratory disease in rhesus macaques inoculated with SARS-CoV-2. *Nature*.

Ogando, N.S., Dalebout, T.J., Zevenhoven-Dobbe, J.C., Limpens, R.W.A.L., van der Meer, Y., Caly, L., Druce, J., de Vries, J.J.C., Kikkert, M., Barcena, M., et al. (2020). SARS-coronavirus-2 replication in Vero E6 cells: Replication kinetics, rapid adaptation and cytopathology. *J. Gen. Virol.* 101, 925–940.

Pierson, T.C., and Diamond, M.S. (2015). A game of numbers: The stoichiometry of antibody-mediated neutralization of flavivirus infection (Elsevier Inc.).

Quicke, K., Gallichotte, E., Sexton, N., Young, M., Janich, A., Gahm, G., Carlton, E.J., Ehrhart, N., and Ebel, G.D. (2020). Longitudinal Surveillance for SARS-CoV-2 RNA Among Asymptomatic Staff in Five Colorado Skilled Nursing Facilities: Epidemiologic, Virologic and Sequence Analysis. *MedRxiv*.

Robb, J.A., and Bond, C.W. (1979). Pathogenic murine coronaviruses I. Characterization of biological behavior in vitro and virus-specific intracellular RNA of strongly neurotropic JHMV and weakly neurotropic A59V viruses. *Virology* 94, 352–370.

Rockx, B., Kuiken, T., Herfst, S., Bestebroer, T., Lamers, M.M., Munnink, B.B.O., De Meulder, D., Van Amerongen, G., Van Den Brand, J., Okba, N.M.A., et al. (2020). Comparative pathogenesis of COVID-19, MERS, and SARS in a nonhuman primate model. *Science* (80-). 368, 1012–1015.

Rogers, T.F., Zhao, F., Huang, D., Beutler, N., Burns, A., He, W.T., Limbo, O., Smith, C., Song, G., Woehl, J., et al. (2020). Isolation of potent SARS-CoV-2 neutralizing antibodies and protection from disease in a small animal model. *Science* (80-). 369, 956–963.

Salje, H., Kiem, C.T., Lefrancq, N., Courtejoie, N., Bosetti, P., Paireau, J., Andronico, A., Hozé, N., Richet, J., Dubost, C.L., et al. (2020). Estimating the burden of SARS-CoV-2 in France. *Science* (80-). 369, 208–211.

Schön, M.P., Berking, C., Biedermann, T., Buhl, T., Erpenbeck, L., Eyerich, K., Eyerich,

S., Ghoreschi, K., Goebeler, M., Ludwig, R.J., et al. (2020). COVID-19 and immunological regulations – from basic and translational aspects to clinical implications. *JDDG - J. Ger. Soc. Dermatology* 18, 795–807.

Sender, R., Fuchs, S., and Milo, R. (2016a). Are We Really Vastly Outnumbered ? Revisiting the Ratio of Bacterial to Host Cells in Humans. *Cell* 164, 337–340.

Sender, R., Fuchs, S., and Milo, R. (2016b). Revised Estimates for the Number of Human and Bacteria Cells in the Body. *PLoS Biol.* 14.

Seydoux, E., Homad, L.J., MacCamy, A.J., Parks, K.R., Hurlburt, N.K., Jennewein, M.F., Akins, N.R., Stuart, A.B., Wan, Y.H., Feng, J., et al. (2020). Analysis of a SARS-CoV-2-Infected Individual Reveals Development of Potent Neutralizing Antibodies with Limited Somatic Mutation. *Immunity* 53, 98-105.e5.

Snyder, W.S., Cook, M.J., Nasset, E.S., Karhausen, L.R., Parry Howells, G., and Tipton, I.H. (1975). Report of the Task Group on Reference Man (Pergamon Press: Oxford).

Stone, K.C., Mercer, R.R., Gehr, P., Stockstill, B., and Crapo, J.D. (1992). Allometric relationships of cell numbers and size in the mammalian lung. *Am. J. Respir. Cell Mol. Biol.* 6, 235–243.

Sungnak, W., Huang, N., Bécavin, C., Berg, M., Queen, R., Litvinukova, M., Talavera-López, C., Maatz, H., Reichart, D., Sampaziotis, F., et al. (2020). SARS-CoV-2 entry factors are highly expressed in nasal epithelial cells together with innate immune genes. *Nat. Med.* 26, 681–687.

Taylor, H.P., Armstrong, S.J., and Dimmock, N.J. (1987). Quantitative relationships between an influenza virus and neutralizing antibody. *Virology* 159, 288–298.

Turoňová, B., Sikora, M., Schürmann, C., Hagen, W.J.H., Welsch, S., Blanc, F.E.C., von Bülow, S., Gecht, M., Bagola, K., Hörner, C., et al. (2020). In situ structural analysis of SARS-CoV-2 spike reveals flexibility mediated by three hinges. *Science* (80-.). 370, 203–208.

Valyaeva, A.A., Zharikova, A.A., Kasianov, A.S., Vassetzky, Y.S., and Sheval, E. V (2020). Lung epithelial stem cells express SARS-CoV-2 entry factors implications for COVID-19. *Biorxiv* 1–19.

WHO (2020). Report of the WHO-China Joint Mission on Coronavirus Disease 2019 (COVID-19). WHO-China Jt. Mission Coronavirus Dis. 2019 2019, 16–24.

Williamson, B.N., Feldmann, F., Schwarz, B., Meade-White, K., Porter, D.P., Schulz, J., van Doremalen, N., Leighton, I., Yinda, C.K., Pérez-Pérez, L., et al. (2020). Clinical benefit of remdesivir in rhesus macaques infected with SARS-CoV-2. *Nature*.

Yao, H., Song, Y., Chen, Y., Wu, N., Xu, J., Sun, C., Zhang, J., Weng, T., Zhang, Z., Wu, Z., et al. (2020). Molecular Architecture of the SARS-CoV-2 Virus. *Cell* 183, 730-738.e13.

Ziegler, C.G.K., Allon, S.J., Nyquist, S.K., Mbanjo, I.M., Miao, V.N., Tzouanas, C.N., Cao, Y., Yousif, A.S., Bals, J., Hauser, B.M., et al. (2020). SARS-CoV-2 Receptor ACE2 Is an Interferon-Stimulated Gene in Human Airway Epithelial Cells and Is Detected in Specific Cell Subsets across Tissues. *Cell* 181, 1016-1035.e19.